

Original article

Lightening of shale oil using high-temperature supercritical CO₂: An experimental study

Xiang Zhou^{1,2,3}*, Huan Li^{1,2}, Fanhua Zeng⁴, Chunsheng Yu^{1,2}, Hong Ouyang², Qi Jiang^{1,2}

¹State Key Laboratory of Oil and Gas Reservoir Geology and Exploitation, Southwest Petroleum University, Chengdu 610500, P. R. China

²Petroleum Engineering School, Southwest Petroleum University, Chengdu 610500, P. R. China

³State Key Laboratory of Geomechanics and Geotechnical Engineering Safety, Institute of Rock and Soil Mechanics, Chinese Academy of Sciences, Wuhan 430071, P. R. China

⁴Energy Systems Engineering, University of Regina, Regina S4S 0A2, Canada

Keywords:

Lightening process
kinetic reaction parameters
supercritical CO₂
shale oil

Cited as:

Zhou, X., Li, H., Zeng, F., Yu, C., Ouyang, H., Jiang, Q. Lightening of shale oil using high-temperature supercritical CO₂: An experimental study. *Advances in Geo-Energy Research*, 2025, 16(2): 99-113.

<https://doi.org/10.46690/ager.2025.05.03>

Abstract:

This paper investigates the influence of reaction atmosphere and operation parameters of the lightening process under high temperature and high pressure on high-viscosity shale oil using an experimental approach. Two types of experiments were implemented, one involving a thermogravimetric analyzer and another using an autoclave to carry out the lightening process. By these two kinds of experiments, the effects of reaction atmosphere and operation parameters on the lightening efficiency were clarified. As for the reaction atmosphere, the effects of CO₂, N₂ and air were separately evaluated. As for the operation parameters, the effects of heating rate and formation rock were investigated. The results indicate that under a CO₂ atmosphere, the lightening reaction is more intense than that under the other two gas phases, and it gains the highest reaction rate. Part of the minerals in the formation rock can be treated as catalyst in the shale oil lightening process. With the formation rock being present, the reaction rate increases significantly and higher contents of light components are obtained in both the lightened shale oil and gas phase. For the kinetic parameters in the lightening process, proportional relationships between the kinetic parameters and heating rates under CO₂ atmosphere with and without formation rock were identified. The findings of this study can provide guidance for enhancing high-viscosity shale oil using an *in-situ* lightening process.

1. Introduction

With the declining production of conventional oil, research on shale oil reserves is increasingly focused on by scholars due to the huge reserves of shale oil was found all over the world (Guo et al., 2024a; Ren et al., 2024). For most shale oil reserves in the western part of China, one of the most significant characteristics is high viscosity and low maturity (Zhao et al., 2018; Feng et al., 2020), which results in a low oil recovery factor using the conventional recovery method. To boost the recovery of high-viscosity shale oil, the high-

temperature Supercritical CO₂ (ScCO₂) injection process has been introduced, which has been proven as one of the most efficient approaches (Shabib-Asl et al., 2020; Yu et al., 2021). In the high-temperature ScCO₂ injection process, the liquid hydrocarbon can be produced mainly by the mechanisms of shale oil lightening, gas drive (Gong and Gu, 2015a), and extraction of light components (Gong and Gu, 2015b; Gao et al., 2021; Zhao et al., 2021). To clarify the mechanisms of shale oil production using the high-temperature ScCO₂ injection process, scholars have conducted various experimental studies evaluating different parameters.

The shale oil lightening process can be described as one where high-temperature gas is injected into the *in-situ* reservoir, resulting in evaporation, oxidation, gasification, pyrolysis etc., so that the high-viscosity shale oil is transferred into light oil and gas phase (Guo et al., 2024a; Wang et al., 2024; Zhao et al., 2024). Under the high-temperature condition, the lightening study of high viscous shale oil was mostly carried out using Thermogravimetric Analyzer (TGA)-Differential Scanning Calorimetry (DSC) (Al-Harashseh et al., 2011; Chang and Chu, 2019; Yang et al., 2022b) and High-Temperature High-Pressure (HTHP) reaction kettle (Chang et al., 2018). In addition, the lightening process was mainly divided into three stages (Moine et al., 2016; Kang et al., 2020). Once the original high-viscosity shale oil has been converted into light oil by lightening, oil in the reservoir will have a higher mobility, and a higher recovery factor can be obtained. The main parameters affecting the shale oil lightening ratios are the temperature of gas atmosphere, heating rate, end-temperature, catalysis, etc. (Gu et al., 2024). As for the heating rate, a previous study indicated that a higher heating rate leads to a higher reaction rate albeit a lower reaction efficiency (Jiang et al., 2023). With the heating rate increasing, the ratios of olefin and alkane among the lightening products also increase in the lightened shale oil (Lan et al., 2015). Some scholars have indicated that by increasing the heating rate, both the active energy and the reaction factor rise in the lightening process (Pan et al., 2015). However, other studies found no relationship between the heating rate and active energy of the lightening process (Syed et al., 2011); therefore, this relationship needs to be further clarified.

The characteristics of the lightening process are different when different gases are applied. These gases can be CO₂, N₂, a mixture of CO₂ and CH₄, natural gas, etc. For various gas phases, although similar oil properties were investigated for both CO₂ and N₂, the molecular structures of the lightened oil were different, and CO₂ could improve the quantity and quality of the derived oils (Mozaffari et al., 2022). In addition, among these heating carriers, CO₂ is the best choice since it can carry a higher amount of heat energy under high pressure and high temperature (Kang et al., 2020). ScCO₂, that is, CO₂ under a temperature higher than 31.1 °C and a pressure higher than 7.38 MPa, has the advantages of high solubility, excellent diffusion (Zhao et al., 2020) and high extraction efficiency (Yu et al., 2021) when used in shale oil recovery (Jin et al., 2017; Jia et al., 2019). When ScCO₂ is utilized in the shale oil lightening process, a higher reactivity of the long chain of the organic compounds can be achieved, leading to a decreased activation energy, so that the energy will be lower and the lightening process can occur easily (Tang et al., 2019).

When high-temperature ScCO₂ is employed in the *in-situ* shale formation, some minerals in the shale rocks are usually treated as catalysts in the lightening process. Generally, previous studies have found that the catalysts enhanced the secondary cracking of shale oil, yielding less oil and more gas (Chang et al., 2017). Moreover, the influences of inherent/additional pyrite were shown to be different, while a positive effect on the production of light oil was observed in inherent pyrite (Gai et al., 2014), whereas additional pyrite boosted the

lightening of oil, thus increasing the gas yield. The presence of minerals in the formation rock, such as the clay minerals, improves the initiation temperature of kerogen cracking, enhancing the conversion ratio under the same temperature condition (Borrego et al., 2000; Al-Harashseh et al., 2011). Some scholars have reported a positive influence of certain minerals on the shale oil lightening process. Meanwhile, others have argued that the presence of minerals does not remarkably influence the lightening process (Pan et al., 2016). To clarify the effect of formation rock minerals on the shale oil lightening process applied in the targeted reservoir, this study employs a shale sample in this process.

The proportion and type of oil components do indeed affect the lightening performance, which has previously been explored by scholars using different high-viscosity oil samples (Hao et al., 2017; Quan and Xing, 2019; Yang et al., 2022b). For example, the analysis of Saturates, Aromatics, Resins, and Asphaltenes (SARA) was performed on oil samples. In our previous study (Yang et al., 2022b), Fourier transform infrared spectrometer spectroscopy tests revealed that the absorption peaks of the studied oil samples were similar, indicating that the chemical bonds and characteristic functional groups were comparable. The experimental results revealed similar lightening processes, with peak temperatures ranging from 425 to 479 °C. The thermal stability of each oil sample is closely related to the fraction of asphaltenes, as they possess the highest thermal stability (Zhang et al., 2015). Consequently, as the fraction of asphaltenes in the oil increases, the TGA plot shifts to the right. Thus, it can be deduced that the key factors influencing the lightening process are the chemical bonds, characteristic functional groups, and the fraction of asphaltenes in the oil sample.

Regarding the chemical reaction stages, the kinetic parameters such as activation energy, frequency factor, reaction order etc., were calculated in the shale oil lightening process. Previous studies have revealed that the reaction order and frequency factor change under different heating rates and stages, as indicated in Table 1. From these data, one can find that the lightening process is feasible for both light oil (with viscosity as low as 12 mPa·s under 20 °C) and bitumen (with viscosity as high as 68,120 mPa·s under 100 °C). Consequently, to boost production in oil reservoirs, the high-temperature ScCO₂ injection process (applying the mechanism of lightening the heavy components into light and medium components) can be applied for both low-viscosity and high-viscosity oil reservoirs. For this process, the reaction order ranges from 0 to 3.94 and the frequency factor ranges from 7.7 to $1.4 \times 10^5 \text{ min}^{-1}$ (Murugan et al., 2012); the activation energy ranges from 200 to 242 kJ/mol, and the frequency factor ranges from 10^{12} to 10^{16} S^{-1} (Raja et al., 2017). The kinetic parameters in the oil lightening process are mainly influenced by the properties of the oil sample, the gas atmosphere and the heating rate. The peak temperature is usually around 450 °C, while it can be as low as 270 °C for Athabasca bitumen and 290 °C for saturates. This is mainly because for saturates, the fraction of the high molecular components is lower than that for resins and aromatics, thus the reaction energy in the decomposition is lower and the peak temperature

Table 1. Calculation of kinetic parameters in the oil lightening process.

Oil sample	Viscosity (mPa·s)	Peak temperature (°C)	Gas atmosphere	Heating rate (°C/min)	Activation energy (KJ/mol)	Frequency factor (min ⁻¹)	Reference
Athabasca bitumen, Canada	7,500 @40 °C	260-465	N ₂	5/10/20	25.3-86.3	7.7-1.4e ⁵	Murugan et al. (2012)
Neilburg field, Canada	1,700 @20 °C	/	N ₂ /Air	10	136.85/131.09	1.93e ⁹ /6.63e ⁸	Ren et al. (2007)
Canada heavy oil	/	444	CO ₂	5/10/20	119-350	/	Yang et al. (2022b)
Cold Lake, Canada	/	/	Air/Wet air	/	0.414-190	21-2.93e ⁶	Kapadia et al. (2013)
Athabasca bitumen, Canada	117,242 @20 °C	270	Air	1.67	176.3-234.7	2.27e ⁷ -1.52e ¹¹	Belgrave et al. (1993)
Bitumen, Italian refiner	68,120 @100 °C	455.9-486.9	Argon	5/10/20/40	Average	258.4 average 5.77e ¹⁷	Maniscalco et al. (2020)
Take Oilfield, China	1.41e ⁵ @25 °C	-	Air	5	20.75-59.29	49.33-1.04e ⁵	Pu et al. (2020)
Shale oil	/	457 with catalyst, 355-451	/	10	113.8 with catalyst, 37.28-51.32	9.52e ¹² with catalyst, 2.30e ¹² -1.56e ¹³	Meng et al. (2020)

is also lower. For Athabasca bitumen, the gas media is air, the decomposition process is combustion, so the peak temperature is low. To date, many studies on the pyrolysis process on oil shale have been conducted using experimental approaches (Jaber and Probert, 1999; Jiang et al., 2017) and numerical simulation methods (Syed et al., 2011; Zhao et al., 2020; Zhou et al., 2022). Nonetheless, the lightening of shale oil has been rarely investigated; therefore, this study mainly focuses on the lightening process of shale oil.

The *in-situ* lightening process is a novel technology, rare field application was investigated in the shale oil reservoir. But this method has been used to lighten the oil shale, achieving an oil recovery factor of nearly 70% in the process (Yang et al., 2022a). This level of recovery demonstrates that lightening can be an effective approach to enhance oil recovery in shale reservoirs. A pilot test of this technology was conducted in the Songliao Basin, China (Guo et al., 2024b). In total, 3,490 L of oil and 18,000 m³ of gas were produced, and the produced oil consisted mostly of light components, over 71% of which were n-alkanes and aromatic hydrocarbons. The success of the pilot test applied in the oil shale indicates a high potential of lightening process in the shale oil reservoir.

In this paper, shale oil lightening experiments were carried out, and the effects of various gas atmospheres, the presence of formation rock, and the heating rate were investigated. The experimental results indicate that for the *in-situ* lightening process, under CO₂ atmosphere, the lightening performance is enhanced and the reaction rate is the highest compared to the other two gas phases. Part of the minerals in the formation rock could yield benefits in the shale oil lightening process, that is, a significantly increased reaction rate and a higher content of light components in both the lightened shale oil and gas

phase. Furthermore, proportional relationships between kinetic parameters and heating rates in CO₂ atmosphere with and without formation rock were established in the lightening process. By means of experimental and mathematical approaches, the mechanisms of shale oil lightening under different gas atmospheres and the influences of various operational parameters were clarified, and the impact of formation rock on the *in-situ* lightening of shale oil was analyzed. Additionally, the kinetic reaction parameters of the lightening process were determined using a mathematical model. The findings of this study can provide valuable guidance for enhanced high-viscosity shale oil recovery using the lightening process.

2. Experimental section

2.1 Materials

The shale oil sample and formation rock were collected from Xinjiang Oilfield, the western part of China. Under surface conditions, the viscosity of shale oil is 2,457 mPa·S and the density is 0.895 g/mL. The components of shale oil sample are listed in Table 2. From these data, one can find that the targeted shale oil mainly includes heavy components (C₁₄₊), up to 76.24%. The purities of the gas media of CO₂ and N₂ are 99.999% and 99.99%, respectively. The components of minerals in the formation rock can be found in Table 3.

2.2 Experimental setup

In this study, two types of experiments were implemented: (1) The shale oil lightening process was applied in TGA under different gas atmospheres; (2) the shale oil lightening process under CO₂ atmosphere was applied in a HTHP autoclave. To investigate the performance of shale oil weight loss and weight

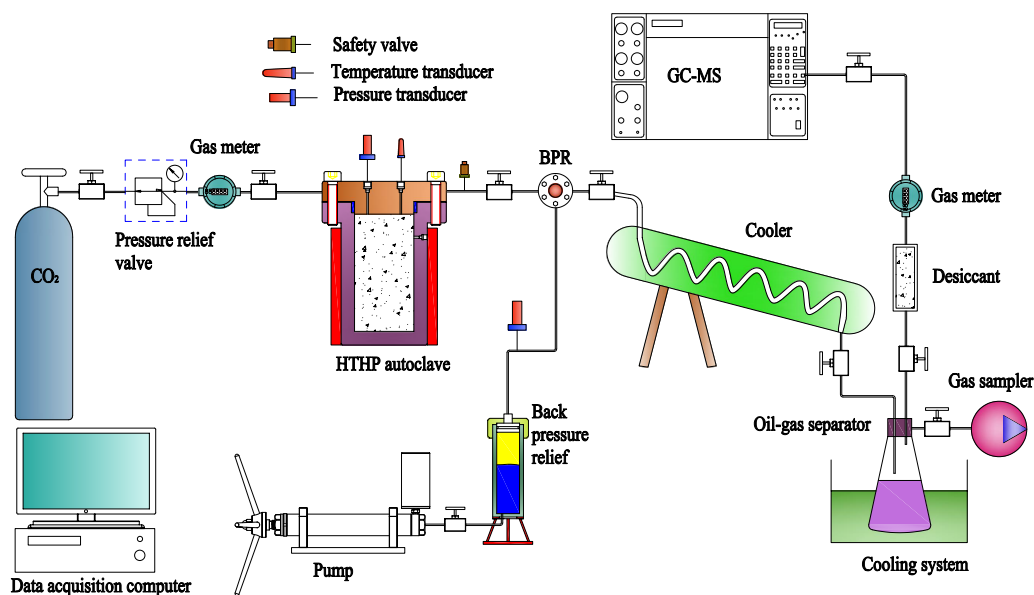


Fig. 1. Experimental setup of the shale oil lightening process using HTHP autoclave.

Table 2. Component analysis of the targeted shale oil.

Components	Mass weight (%)	Components	Mass weight (%)
nC ₆	2.02	nC ₂₀	4.90
nC ₇	2.67	nC ₂₁	5.30
nC ₈	3.22	nC ₂₂	4.83
nC ₉	2.97	nC ₂₃	5.07
nC ₁₀	3.09	nC ₂₄	3.88
nC ₁₁	3.19	nC ₂₅	4.06
nC ₁₂	3.09	nC ₂₆	2.98
nC ₁₃	3.52	nC ₂₇	2.84
nC ₁₄	3.90	nC ₂₈	1.93
nC ₁₅	4.25	nC ₂₉	1.97
nC ₁₆	4.20	nC ₃₀	1.03
nC ₁₇	5.04	nC ₃₁	1.35
nC ₁₈	4.33	nC ₃₂	8.70
nC ₁₉	5.68	Sum	100.00

loss ratio under different gas atmospheres, a TGA (Mettler Toledo, TGA/DSC 3+) with a mass weight accuracy of 0.0025% and a heating rate of up to 250 °C/min was employed. The setup of the TGA is referred to a previous study (Yang et al., 2022b). The experimental setup of the HTHP autoclave mainly includes three systems, namely, injection system, reaction system and production system, as shown in Fig. 1. The injection system consists of a CO₂ gas cell and a gas volume meter. The reaction system includes a self-created autoclave that can withstand a pressure up to 100 MPa and a temperature up to 900 °C, temperature and pressure transducers, a back pressure regulator that can withstand a pressure of

70 MPa, a pump, and a back pressure relief cell to pressurize the autoclave. The production system uses a cooler to reduce the temperature of the produced gas. An oil-gas separator is used to separate the gas and liquid phases, and a desiccant cell is used to dry the gas phase. Gas Chromatography (GC)-Mass Spectrometry (MS) were implemented to determine the gas compositions in the produced gas phase.

2.3 Experimental procedure

In the lightening process applied in the TGA, 10 experiments were implemented, including 7 experiments to investigate the influence of gas atmosphere (3 experiments in CO₂/N₂ atmosphere and 1 experiment in air atmosphere), and 3 experiments with shale oil and formation rock present in a CO₂ atmosphere. The experimental procedure can be summarized as follows:

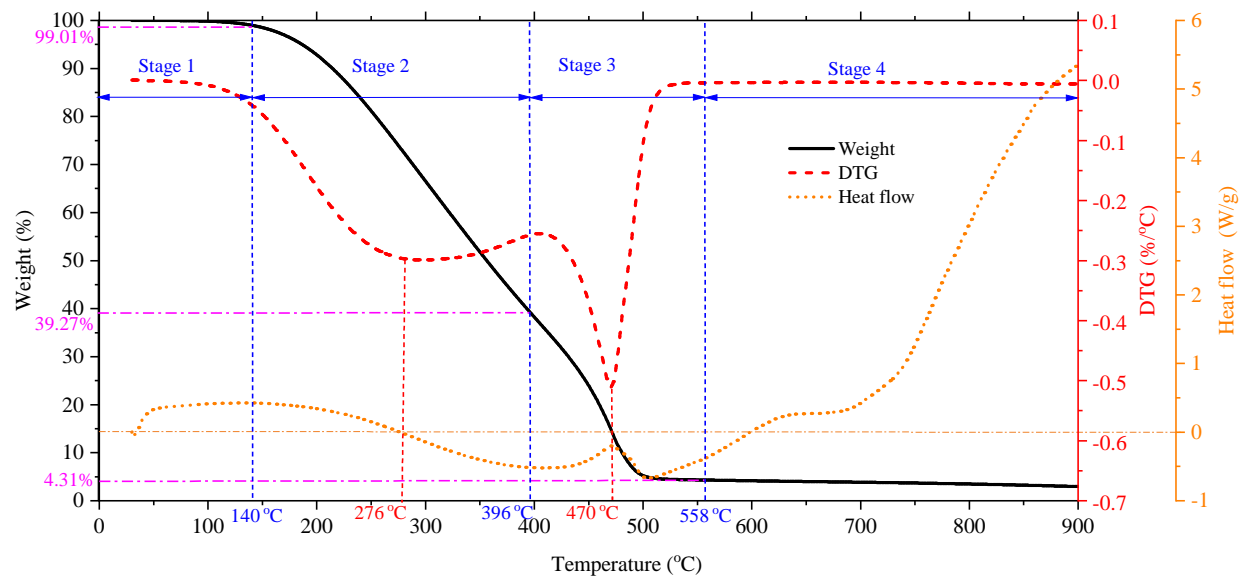
- 1) 10 mg of shale oil was placed in the high temperature cell in the TGA, and the TGA cell was flooded using N₂.
- 2) Gas phases (CO₂, N₂ and air) were introduced into the TGA under an injection rate of 1 cc/min to maintain the designed gas atmosphere.
- 3) The lightening processes in the TGA were carried out under different heating rates (5, 10 and 20 °C/min).
- 4) The characteristics of the shale oil weight loss and weight loss ratios under different gas atmosphere were studied.

Considering the shale oil lightening process applied in the autoclave, experiments were implemented in a CO₂ atmosphere with shale oil, and with a mixture of shale oil and formation rock. To mimic the oil saturation (70%) in the shale oil reservoir, the volume ratio of shale oil and water were 70% and 30% in the liquid phase. The procedures were carried out as follows:

- 1) Certain amounts of different media, such as (a) 70 mL

Table 3. Component analysis of the targeted shale oil.

Mineral	Clay	Barite	Quartz	Potassium feldspar	Plagioclase	Calcite	Dolomite
Content (%)	0.838	4.477	23.355	12.308	33.994	4.329	20.699

**Fig. 2.** Lightening process of shale oil in TGA under the high-temperature ScCO₂ condition.

shale oil and 30 mL brine, (b) 70 mL of shale oil and 30 mL of brine, and 30 g of shale rock powder, were introduced into the autoclave, respectively. Then, the autoclave was vacuumed for at least 4 hours to make sure that no air present in the autoclave could affect the experiments.

- CO₂ was injected into the autoclave to maintain the pressure up to 1 MPa at room temperature.
- The autoclave was heated up to 500 °C, then the temperature was kept for 24 h.
- The compositions of gas and oil after the lightening process were measured.

3. Results and discussion

3.1 Characteristics of shale oil lightening

In this study, the shale oil lightening experiments in the TGA were performed under different heating rates (5, 10 and 20 °C/min). The performances of the shale oil lightening process under the heating rate of 20 °C/min in a CO₂ atmosphere were indicated in Fig. 2. From the data, the shale oil lightening process can be divided into four main stages. In Stage 1, when the heating process begins, the water phase in the shale oil is evaporated at high temperature (Syed et al., 2011; Kang et al., 2020; Yang et al., 2022b) until it reaches around 140 °C. The weight plot remains almost straight, and a slight drop in the slope can be seen. In total, the weight loss ratio is 0.99% in this stage. Due to relatively lower temperature gained in this stage, only unseparated water in the shale oil was evaporated, leading to almost no changes of the weight plot. From the heat

flow plot, one can find that the heat generated in Stage 1 can support the water evaporation process.

In Stage 2, the weight plot and Differential Thermogravimetric (DTG) plot decreases, mainly because in the shale oil, the gas phase, low/middle-molecular components and aromatic hydrocarbons dissolved in the shale oil evaporate (Jaber and Probert, 1999; Kang et al., 2020). The peak temperature is around 276 °C, at which the summit weight loss rate is obtained in this stage. The heat flow transfers from positive to negative, meaning that the heat generated under high temperature is applied in the decomposition of heavy components, liquid evaporation, etc. This trend is different from that obtained in our previous study (Yang et al., 2022b). The reason is that the oil sample used in our previous study was extra heavy oil in which the amount of light components was smaller than that in shale oil, thus the DTG curve was smoother. In this stage, the temperature reached up to 396 °C and the weight loss ratio was up to 59.74%. The reactions in Stages 1 and 2 are mainly physical reactions, and the main products include water and low molecular components (mainly including methane, ethane, propane and butane) (Xie et al., 2010).

In Stage 3, when the temperature in the system reaches 396 °C, the lightening reaction process occurs. The reaction area extends up to 558 °C and the peak temperature is 470 °C. Compared with Stage 2, the reaction range is much smaller, which trend is similar to those in previous studies (Yuan et al., 2018; Jaber et al., 2000; Yang et al., 2022a). The C–C bond in the high molecular components is broken (He et al., 2022), so these components are cracked into gaseous light

hydrocarbons. In addition, the ratios of methane, hydrogen, ethane, etc. in the produced gases are boosted, with a weight loss ratio of 34.96%. The generated energy is mainly used to support the decomposition process, leading to negative heat flow value in this stage. The weight loss peak in the DTG curve reaches $0.51\%/^{\circ}\text{C}$, meaning that the weight loss ratio is lower than that in heavy oil (the weight loss peak is $0.72\%/^{\circ}\text{C}$). This is mainly because in our previous study (Yang et al., 2022b), the oil sample, which was collected from Canada, contains 45.56 wt% of resins and asphaltene, much higher than that in the targeted shale oil sample. The main components cracked into low molecular components are asphaltene and resins (Kök and Karacan, 1998; Alvarez et al., 2011), so that the cracking rate is relatively lower in this study.

In Stage 4, the coke generated in Stage 3 is dehydrogenated. The temperature ranges from 558 to 900°C , although it is much higher than that in other stages, but the weight loss ratio is much lower. The weight in the thermogravimetric (TG) curve for 558 and 900°C are 4.31% and 2.96%, respectively, so the weight loss ratio in this stage is only 1.35%, which is mainly due to two reasons: (1) The main weight loss is hydrogen, the ratio of components increases with the temperature rising, and the other gaseous components (methane, ethane, etc.) are much lower in the produced gas phase in this stage (Yang et al., 2022b). (2) The weight of the hydrogen generated from the coke is small. When the temperature in the system is heated up to 900°C , the DTG curve is almost stable at 0, which means that the coke generated in Stage 3 cannot be further dehydrogenated. In this stage, the heat flow plot rises to a positive value and then keeps increasing to 5.35 W/g. This indicates that most part of the energy generated at high temperature is lost rather than used for the decomposition of high molecular components, because of the ratio of high molecular components left is much lower than that in the former stages, thus no more energy is needed in the decomposition process.

3.2 Effects of operation parameters

3.2.1 Gas atmosphere

In the shale oil lightening process, the gas atmosphere remarkably affects the decomposition efficiency (Liu et al., 2017). In this research, the study on the influence of gas atmosphere (CO_2 , N_2 , and air) was implemented using a TGA. The TG and DTG plots of shale oil under a heating rate of $20^{\circ}\text{C}/\text{min}$ can be seen in Fig. 3. From the data, one can find that in the CO_2 atmosphere, the weight of the shale oil sample decreases with the temperature increasing due to decomposition in the lightening process. Under a temperature of 200°C , the evaporation of water phase and light components is slower than that in other gas atmospheres. This may be because the specific heat capacity of CO_2 is relatively lower than that of N_2 and air, so that the heating rate in CO_2 is lower. For the high molecular decomposition process, which occurs in Stages 2 and 3, the lightening rate is much higher for the shale oil in the CO_2 atmosphere than that in the other two types of gases.

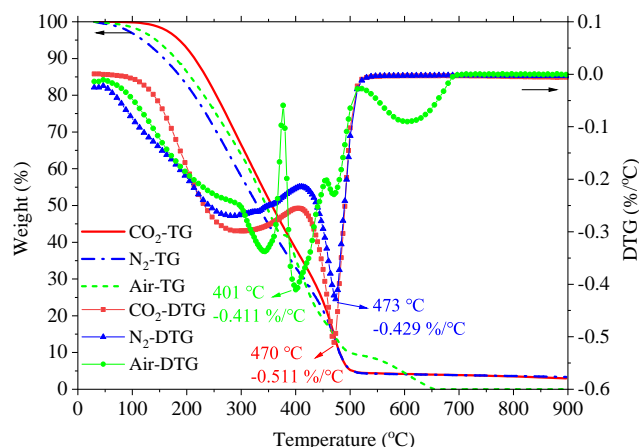


Fig. 3. TG and DTG plots for shale oil lightening in different gas atmospheres.

For the shale oil lightening process in air atmosphere, the oxidation process can be divided into three stages, including evaporation, low-temperature oxidation, and high-temperature oxidation (Liu et al., 2019). Due to the complex lightening process of shale oil, the trends in our experiments were not clear, similar to previous studies (Ren et al., 2007; Liu et al., 2019). When the temperature increased to around 350°C , the first peak of DTG plot appeared. Four summits were investigated in this plot; the weight loss rate was relatively higher than that in the other two gases, and the highest weight loss rate in the plot moved to a lower-temperature area. This is mainly because for the CO_2 and N_2 atmospheres, the weight loss of the shale oil is essentially due to the oil decomposition process. However, in air atmosphere, because of the exiting of O_2 , a higher reaction rate of shale oil occurs under high temperature, leading to a higher weight loss rate and lower burning temperature. When the highest weight loss rate reaches 401°C , the weight loss ratio of the shale oil in air atmosphere is 64.98%, but for the other two gases, over 80% of the shale oil has decomposed when the highest weight loss rate is obtained at around 470°C . Therefore, the main decomposition stages in the air atmosphere are moved forward to a relative lower-temperature area. In the later stage, a second lightening process was obviously investigated in the air atmosphere between 500 to 700°C , but this phenomenon was not observed in the other two gas atmospheres. This is mainly because in the lightening process with N_2 and CO_2 , the C–C bond in the high molecular components are mainly broken before the temperature reaches 470°C , and the solid carbon is left after the lightening process. Therefore, the weight plot for N_2 and CO_2 atmosphere reaches 3.33% and 2.96%, respectively. In the CO_2 atmosphere, CO_2 increases the hydrocarbons in the produced liquids, due to CO_2 providing C and promoting the H component free radical. In this way, the hydrocarbons in the produced liquids are boosted, so the weight loss ratio is higher than other two gas atmospheres.

3.2.2 Formation rock

When high-temperature ScCO_2 is employed into the reservoir, some special minerals (which can be treated as catalyst)

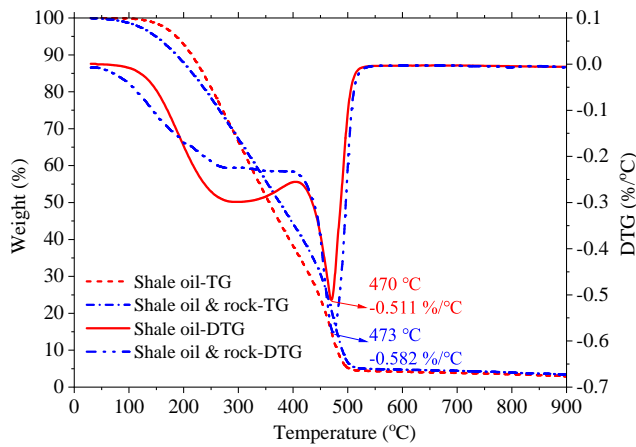


Fig. 4. Lightening performance of shale oil with/without formation rock.

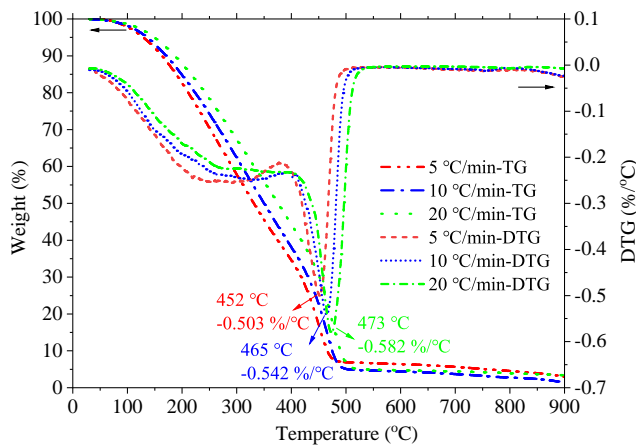


Fig. 5. Performance of shale oil lightening process under different heating rates with formation rock.

in the formation significantly affect the decomposition process (Borrego et al., 2000; Al-Harshesh et al., 2011; Pan et al., 2016). To investigate the influence of formation rock in the lightening process, the formation rock was included in the experiments. The rock was collected from the targeted shale reservoir and mashed into powder. Around 10 mg shale oil and 10 mg rock were employed, and they were mixed uniformly. The heating rates were 5, 10 and 20 °C/min, respectively. Take the heating rate of 20 °C/min as an example, the lightening performances of shale oil with/without rock powders can be found in Fig. 4. From the data, one can find that in the lower-temperature region, the weight loss rate is higher in the shale oil with rock, due to the thermal conductivity of rock being higher than that of the shale oil. The heat transfer rate is also higher, the inner temperature of the rock and shale oil mixture is higher at the same time, and the evaporation of light components and water phase is more obvious. Thus, the weight plot is lower for the rock and shale oil mixture.

Once the decomposition process has occurred under high temperature, the cracking of the C-C bond in the higher-molecule components occurs on the surface of shale oil. Since the rock in the shale oil occupies part of the surface of the mixture, it results in the decomposition rate being lower than

that in the pure shale oil in a temperature range of 200 to 430 °C. However, at higher temperature, parts of the minerals in the rock act as catalysts. With the effect of rock, the reaction rate increases significantly in the mixture of rock and shale oil, and the highest reaction rate reaches 0.582%/°C at 473 °C. The reaction area moves slightly to the higher temperature region, and the highest lightening rate changes from 470 to 473 °C. These phenomena are different from that in a previous study (Meng et al., 2020). The reasons might be that the tests with pure catalyst were applied in the low- and medium-maturity shale oil, the reaction area moved to a lower temperature area or was similar to the lightening process without catalyst, and different catalysts indicate various lightening performances. The temperature at which the mass starts to decrease was achieved changed from 6 to 102 °C forward to a range similar to the shale oil decomposition process without catalyst. There are several main reasons for this difference:

- 1) The maturity of shale oil applied in this study was different from those in previous ones;
- 2) The amount of minerals that can be treated as catalyst were small in the targeted rock;
- 3) The clay and solid materials in the rock powders reduced the surface area of the shale oil, exerting a negative influence on the lightening process;
- 4) Under a relatively higher heating rate, the heat process was delayed because the temperature increased quicker than that under a lower heating rate.

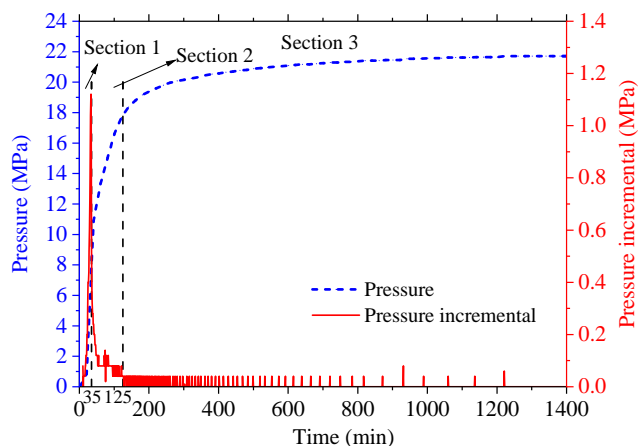
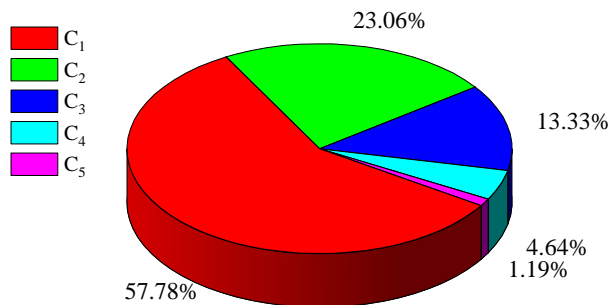
3.2.3 Heating rate

In order to investigate the effects of heating rate on the lightening process of shale oil with the shale rock present, heating rates of 5, 10 and 20 °C/min were implemented with the formation rock. Taking the lightening process carried out in a CO₂ atmosphere as an example, the performances were shown in Fig. 5. From the results, one can find that for different heating rates, similar trends in the TG plots are observed. As the heating rate increases, the TG plots for shale oil with rock shift to higher temperatures. This is mainly because in the lightening process, heat is transferred from the outside to the inner part of the shale oil. At a lower heating rate, the temperature of the inner shale oil increases more evenly, leading to a more gradual evaporation process. As a result, the TG plot is lower in the lower temperature range, which leads to a lower lightening start temperature. Once the higher temperature areas are reached, the temperature at which the highest lightening rates are obtained moves from 452 to 465 °C, and the lightening rate increases from 0.503 to 0.582 %/°C, under a heating rate increasing from 5 to 20 °C/min. This is mainly because (1) the heat transformation rate rises with the heating rate increasing; (2) the explosion time of shale oil is relatively shorter under a lower heating rate; (3) the frequency factor of the reaction is higher under a higher heating rate. On the contrary, under a higher heating rate, the temperature difference between the outside and inside of shale oil is greater, thus it exerts a negative effect on the lightening process.

In this study, the shale oil lightening process was performed

Table 4. Parameters of shale oil lightening in different gas atmospheres.

Gas atmosphere + Oil sample	Heating rate (°C/min)	Lightening range (°C)	Highest lightening rate temperature (°C)	Highest lightening rate (%/°C)
CO ₂ + Shale oil	5	381-509	443	0.3814
	10	393-523	449	0.4299
	20	406-544	470	0.5109
CO ₂ + Shale oil with rock	5	385-500	452	0.5027
	10	409-512	465	0.5421
	20	417-535	473	0.5816
N ₂ + Shale Oil	5	380-521	448	0.3982
	10	395-530	462	0.4267
	20	410-546	473	0.4289

**Fig. 6.** Pressure changes of the lightening process in the autoclave.**Fig. 7.** Components of the produced gas during the lightening process.

under CO₂ and N₂ atmospheres with/without rock. The results showed that the start/end temperature and the highest lightening rate increases with the heating rate, as listed in Table 4. This can be explained by two reasons: (1) A higher heating rate leads to less even heat distribution within the shale oil, causing the reaction to occur at higher temperatures; and (2) a higher heating rate increases the frequency factors in the lightening process, thereby boosting the reaction rate. As

shown in Table 4, the presence of formation rock significantly increases the highest lightening rates under different heating rates due to the catalytic effect of the minerals in the rock. The duration of the main lightening process is shorter than that without rock, thus the lightening range is reduced. However, the highest lightening rate temperature increases to 3 to 13 °C compared to the sample without formation rock, which is mainly because the rock in the mixture has both beneficial and negative influences on the shale oil lightening process. As for the beneficial effect, some of the minerals act as catalysts in the lightening process. As for the negative effect, the powders present as an obstacle for the heat and CO₂ transferred into the shale oil, resulting in a highest lightening rate temperature that is achieved relatively later. The lightening area for the CO₂ atmosphere is lower than that applied in the N₂ atmosphere, as CO₂ is a better heat carrier than N₂.

3.3 Lightening process in the autoclave under in-situ reservoir conditions

In the shale oil lightening process under a ScCO₂ atmosphere, the high molecular components in shale oil can be cracked into low molecular components and gas phase (Bagci and Kok, 2004; Yang et al., 2022b). In this study, the lightening performance was investigated using an autoclave with pure shale oil, and a mixture of rock and shale oil, respectively.

3.3.1 Lightening performance of shale oil

In order to investigate the shale oil lightening performance, the autoclave was used to conduct shale oil lightening experiments at 470 °C (the highest lightening rate temperature) under CO₂ atmosphere. The components of the oil samples before and after the lightening process were measured, and the components of the produced gas in the lightening process were analyzed.

The pressure changes of the lightening process can be seen in Fig. 6. From the data, one can find that the lightening process can be divided into three sections. For Section 1 (the first 35 min), the pressure in the autoclave is boosted due to

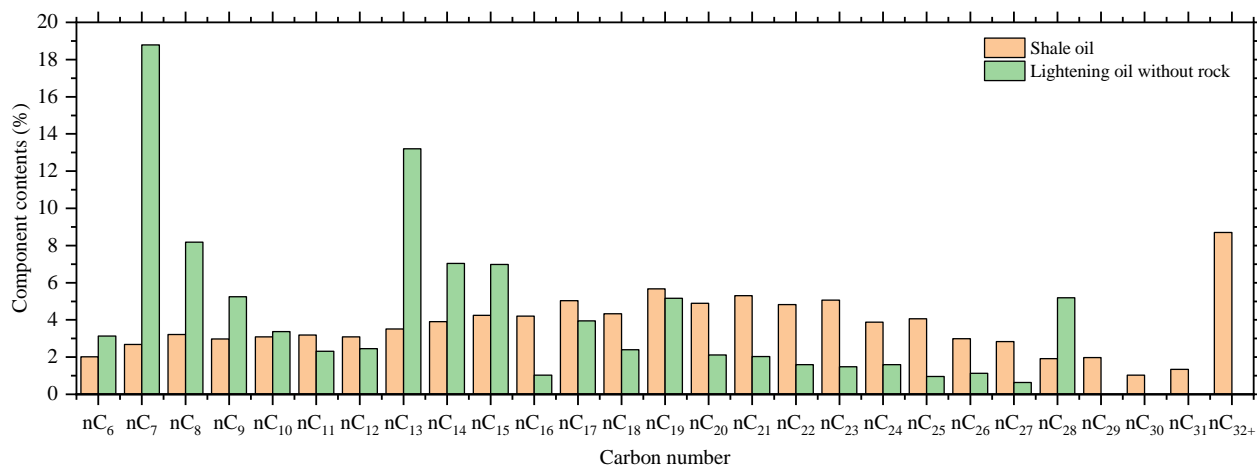


Fig. 8. Components of shale oil before and after the lightening process.

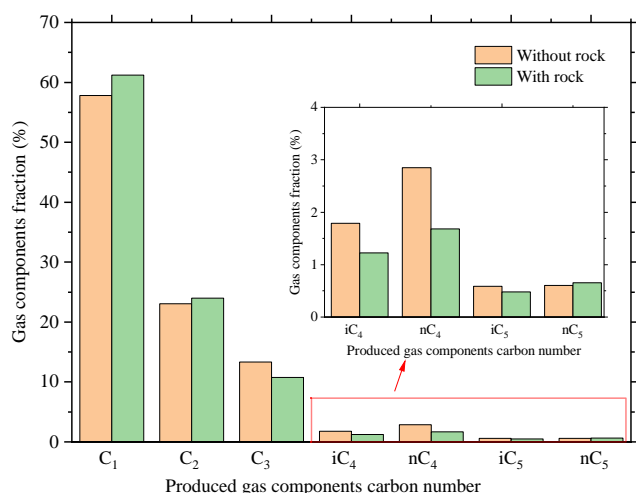


Fig. 9. Produced gas components with/without formation rock in the lightening process.

the increasing temperature in the autoclave, so that the water and relatively light components in the shale oil evaporate, leading to the highest increment in pressure, reaching up to 10.68 MPa. In this section, it is mainly the physical reactions that occur. For Section 2, the pressure keeps increasing but the pressure incremental ratio declines. This is because the evaporation process is completed and the high molecular components start to break into low molecular components. The volume increase in the lightened low molecular components is smaller than that in the evaporation process, resulting in the incremental decrease in pressure. In this stage, the lightening reaction is mainly carried out and the pressure reaches up to 17.60 MPa at the end. For Section 3, the pressure increases slowly because the reaction process essentially occurs, with the reactions mainly being asphaltene decomposition at the end of the lightening process (Eletsii et al., 2018), such that the amount of generated gas is low. Once the pressure reaches a constant value, the test is ended, with the final pressure reaching up to 21.7 MPa.

After the lightening process, the generated gas phase and solid carbon (coke) are observed, as indicated in Fig. 7. From

the data, one can find that the main parts of the gas phases are methane and ethane, and the fraction of these two components is 80.84%. In the high-temperature ScCO_2 atmosphere, the long C–C bond in the oil phase is broken into a relatively shorter C–C bond. Thus, the mobility of the shale oil is extremely enhanced after the lightening process. Subsequently, however, the coke is generated mainly from asphaltene in the shale oil under high temperature (Kim and Lee, 2019). This coke is stuck to the inner surface of the autoclave, from where it can be collected.

When performing the shale oil lightening process in the HTHP autoclave, the components of shale oil before and after the lightening process were compared, as indicated in Fig. 8. The component contents of the relative medium and high molecular components in the shale oil decreased remarkably for C_{16+} , especially for the components of C_{20+} . This is mainly because at high temperature, the high molecular components were cracked into low and medium molecular components, such that the components of C_{28+} were significantly decreased. Therefore, the contents of C_7 , C_8 , C_9 , C_{13} , C_{14} , C_{15} were extremely boosted, resulting in the modification of properties of the shale oil such as viscosity, density, etc., leading to the enhanced mobility of the lightened shale oil in the reservoir and yielding a higher oil recovery factor.

3.3.2 Lightening performance in the presence of formation rock

In order to mimic the shale oil lightening process taking place in the *in-situ* shale oil reservoir, the formation rock was introduced into the autoclave along with shale oil, water and CO_2 . Because parts of the minerals in the rock act as catalysts, both the reaction rate and the efficiency are increased in the lightening process (Meng et al., 2020), therefore the gas production is enhanced, as indicated in Fig. 9. From the figure, one can find that the fractions of methane and ethane are higher in the produced gas in the presence of formation rock. Under the effect of catalyst, the C–C bonds in high molecular oil components are broken easier and the activation energy is decreased (Meng et al., 2020), thus higher fractions of methane and ethane are found in the gas phase.

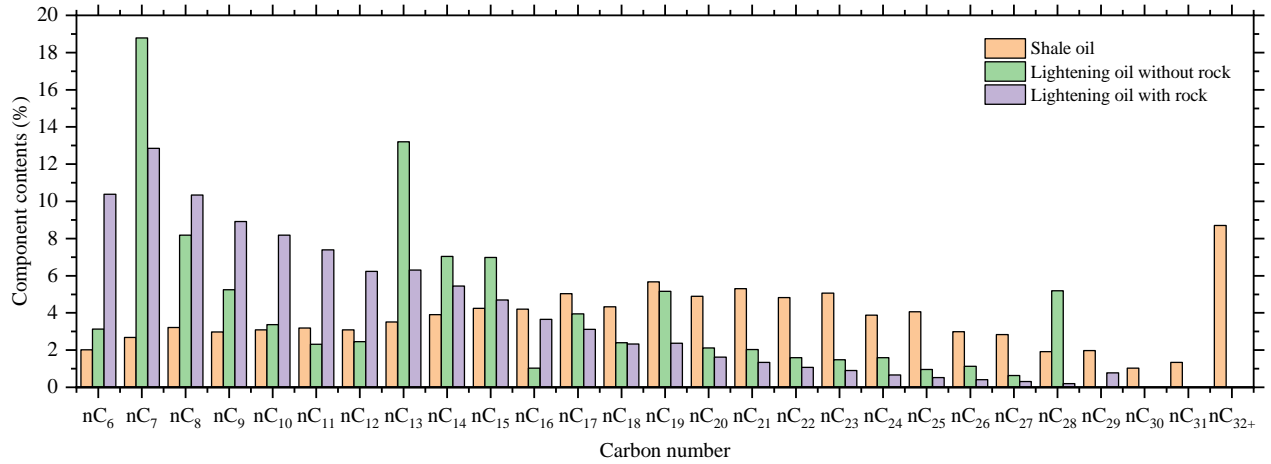


Fig. 10. Components of shale oils before and after the lightening process.

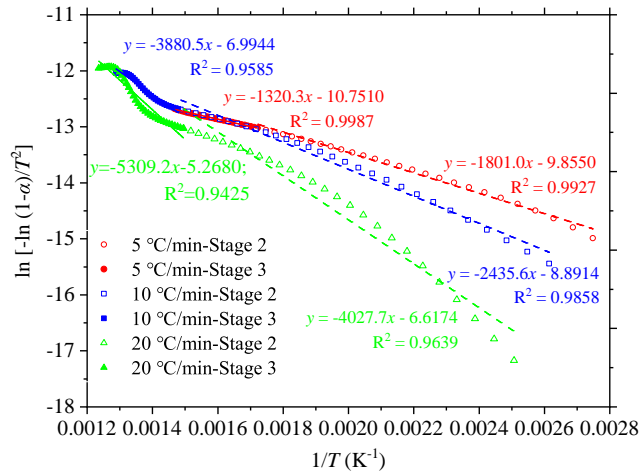


Fig. 11. Relation of $\ln[-\ln(1-\alpha)/T^2]$ and $1/T$ in the chemical reaction stages for the shale oil lightening process under CO_2 atmosphere.

Under the effect of rock, the contents of high molecular components were significantly decreased, as shown in Fig. 10. This is mainly because after lightening, C_{16} and higher molecular components are cracked into relatively low molecular components, that is, the lightening process mainly affect the high molecular components in the shale oil, and under high temperature, the long chain C–C bonds are cracked into short chains (Jiang et al., 2023), so that the contents of the low/middle molecular components increase.

3.4 Determination of lightening kinetic parameters

In this paper, to determine the kinetic parameters of the shale oil lightening process, chemical reaction laws were applied. In the chemical reaction process, the reaction rate of the lightening process applied in shale oil can be expressed as follows (Williams and Ahamad, 2000; Moine et al., 2016):

$$\frac{d\alpha}{dt} = k(T)f(\alpha) \quad (1)$$

$$\alpha = \frac{m_0 - m_t}{m_0 - m_f} \quad (2)$$

where α denotes the conversion ratio of shale oil, dimensionless; t denotes the reaction time, s; T denotes the reaction temperature, K; m_0 denotes the initial weight of shale oil sample, mg; m_t denotes the weight of shale oil sample at time t , mg; m_f denotes the weight of shale oil sample at the end of the reaction process, mg.

The $k(T)$ can be determined using the Arrhenius equation:

$$k(T) = Ae^{-\frac{E_a}{RT}} \quad (3)$$

where A denotes the pre-exponential factor, s^{-1} ; E_a denotes the activation energy, $\text{KJ}\cdot\text{mol}^{-1}$; R is universal gas constant, $R = 8.3145 \text{ J}\cdot\text{mol}\cdot\text{K}^{-1}$.

The $f(\alpha)$ can be gained using the simplified equation:

$$f(\alpha) = (1 - \alpha)^n \quad (4)$$

where n represents the reaction order, which can be determined using the line fitting-method. The temperature rate can be described as $\beta = dT/dt$. Therefore, the equation can be transformed into the following form:

$$\frac{d\alpha}{dT} = \frac{A}{\beta} e^{-\frac{E_a}{RT}} (1 - \alpha)^n \quad (5)$$

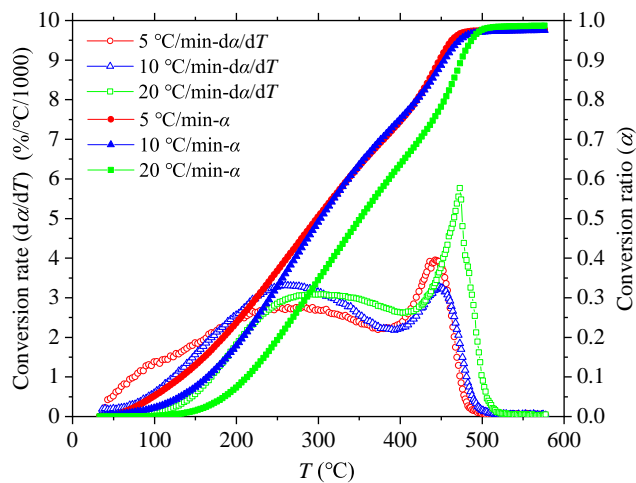
The solution of the equation can be drawn by the Coats-Redfern method (Coats and Redfern, 1964) for the one-order reaction ($n = 1$):

$$\ln\left[\frac{-\ln(1-\alpha)}{T^2}\right] = \ln\frac{AR}{\beta E_a} - \frac{E_a}{RT} \quad (6)$$

From the upper two equations, a linear relationship between $\ln[-\ln(1-\alpha)/T^2]$ and $1/T$ is obtained. Once the plots are developed, the A and E_a values can be obtained by the intercept and slope of the plots, respectively. The experiments of shale oil lightening process in the CO_2 atmosphere were taken as an example to determine the kinetic reaction parameters, as indicated in Fig. 11. For the key reaction stages (Stage 2 and Stage 3), with different heating rates, a linear relationship of $\ln[-\ln(1-\alpha)/T^2]$ and $1/T$ was gained for different stages. The R^2 values for Stage 2 are higher than those for Stage 3,

Table 5. Kinetic parameters of Stages 2 and 3 in the lightening process.

Lightening process	Heating rate (°C/min)	Activation energy (KJ/mol)		Pre-exponential factor	
		Stage 2	Stage 3	Stage 2	Stage 3
Without rock under CO ₂ atmosphere	5	14.97	22.13	0.47	2.42
	10	20.25	32.26	3.35	35.58
	20	33.49	44.14	107.69	547.26
With rock under CO ₂ atmosphere	5	16.54	39.79	0.66	68.93
	10	17.21	49.02	0.91	653.15
	20	17.47	53.70	1.99	2,697.72
Without rock under N ₂ atmosphere	5	21.56	21.74	2.84	2.14
	10	17.27	42.04	1.39	214.53
	20	15.37	47.16	1.57	985.76

**Fig. 12.** Conversion rate of shale oil under different heating rates.

mainly because the main chemical reactions took place in Stage 3, leading to complex reactions such as decomposition, high temperature oxidation, gasification, etc. (Zhou et al., 2021; Zhao et al., 2022; Ogbonnaya et al., 2024). Therefore, the conversion ratio shows various changes and the linear relationship cannot be smooth.

According to the above relationship, the average kinetic parameters of Stages 2 and 3 in the lightening process under CO₂ and N₂ atmosphere with and without rock were determined, as indicated in Table 5. From these data, one can find proportional relationships between kinetic parameters and heating rates for the lightening process in CO₂ atmosphere with and without rock. This is because when the heating rate is increased, the reaction rate also increases and the ratio of heavy components in the shale oil are lightened and the ratio of light components is boosted, resulting in a greater kinetic parameter in the experiment with a higher heating rate. The kinetic parameters in Stage 3 are greater than those in Stage 2, due to the fact that in Stage 2, the evaporation of light components, cracking of

functional groups with lower chemical-thermal-stability, and low-temperature oxidation of shale oil mainly occur. In Stage 3, the cracking of heavy components into light components mainly takes place, and the energy is used to cut the chemical bonds of shale oil, such as the long-chain and side-chain C-C bonds, so that the kinetic parameters are higher than those in Stage 2. However, for the shale oil lightening process under N₂ atmosphere, different trends were found: In Stage 2, the kinetic parameters decreased with the heating rates, but for Stage 3, an inverse relationship was obtained.

During the shale oil lightening process, the conversion ratio (defined as the amount of shale oil was lightened over the total shale oil) and conversion rate (defined as conversion ratio changing within unit temperature) under CO₂ atmosphere were indicated in Fig. 12. From these data, one can find that the relative proportional relationship between the conversion ratio (α) and reaction temperature can be gained; with the temperature increasing, the reactions change from physical reaction to chemical reaction, and the lightened amount of shale oil increases, so that the conversion ratio increases with the reaction temperature. Under different heating rates and the same temperature, an inversely proportional relationship between the conversion ratio and the heating rate was obtained. Since the inner temperature cannot be boosted as high as that outside the shale oil, this leads to the inner reaction undergoing later than that of the outer reaction, so that the conversion ratio is relatively lower. Under a lower reaction temperature, the conversion rate is low, which is mainly due to the fact that under this reaction area, a physical reaction mainly occurs and the water phase is evaporated from the oil sample, so the oil sample is hardly modified. With the reaction temperature increasing, a chemical reaction occurs, so that the shale oil is converted to relative lighter components and the conversion rate of the shale oil is boosted. This mainly happens in Stages 2 and 3, because of the lightening process mainly occurs in these stages, leading to higher reaction rates.

According to Friedman and Carroll's approach (Pan et al., 2015), the relationship of $d\alpha/dT$ vs. $1/T$ with different

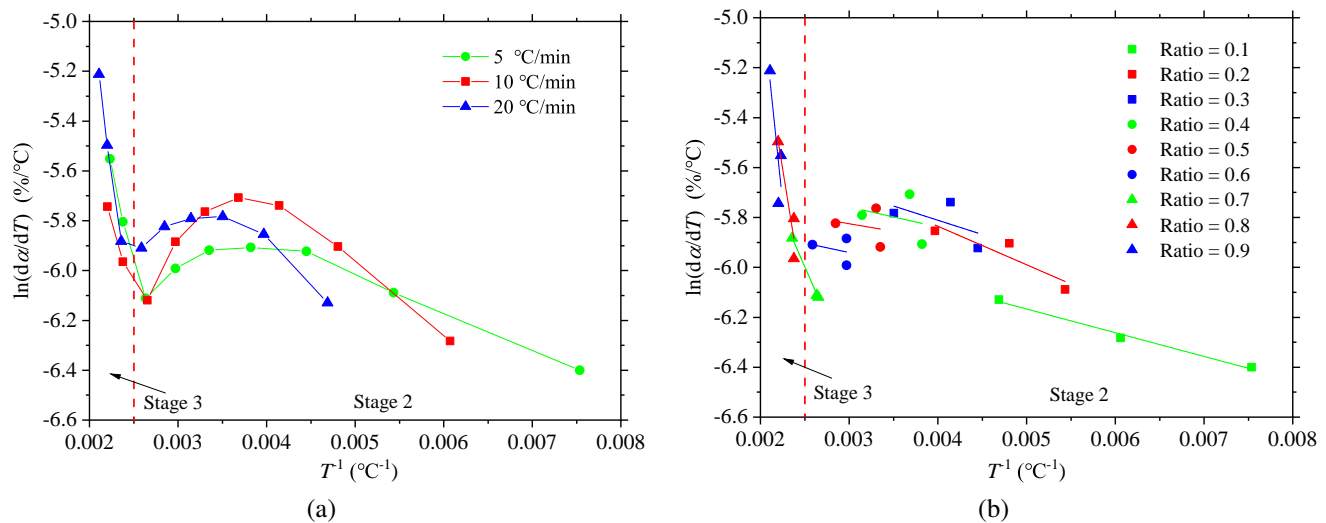


Fig. 13. Relationship of $\ln(d\alpha/dT)$ vs. $1/T$ with different convention ratios for shale oil lightening process under ScCO_2 : (a) Relation for different heating rates and (b) relation for different conversion ratios.

convention ratios were determined, as shown in Fig. 13. From Fig. 13(a), in Stage 2, the conversion rate ($d\alpha/dT$) increases with the temperature rising (the conversion ratio ranges from 0.1 to 0.3), then it decreases slightly (the conversion ratio ranges from 0.4 to 0.7). This is mainly because with the temperature increasing, the physical evaporation of relatively low components and a chemical reaction such as low temperature oxidation occurs, leading to the increased conversion rate in the lightening process. The conversion rate decreases slightly after the conversion ratio reaches up to 0.4, mainly because there are less light/medium components of shale oil that can be evaporated and oxidized at low temperature, and the reaction rate becomes slightly lower, up to a conversion ratio of 0.7. For the lightening process in Stage 3, the conversion rate is boosted significantly, mainly due to the lightening process that has taken place; relatively high components are cracked into low components under high temperature, and the reaction process becomes intense, with this stage being the key chemical reaction stage (Yang et al., 2022), leading to the reaction rate being much higher than that under lower temperature. The conversion rates for different conversion ratio are shown in Fig. 13(b). With different heating rates in Stage 2, the conversion ratio ranges from 0.1 to 0.7, and with the same conversion ratio, the conversion rates are similar. Once the lightening process reaches Stage 3, the conversion rate changes remarkably with the heating rate, and a linear relationship is observed.

The lightening process of shale oil is a new approach for enhanced shale oil recovery, however, the application of this method in the oil field has not been reported. Many researches were conducted at the laboratory scale (Guo et al., 2022; Zhao et al., 2024). Based on the previous studeis, several aspects can be studied in the future, such as:

- 1) The effect of each single mineral in the formation rock;
- 2) Property modification of the shale formation in the lightening process;

- 3) Reactions of water- CO_2 -rock under high temperature, during the lightening process;
- 4) Under the couple influences of Thermo-Hydro-Mechanical-Chemical (T-H-M-C), the reaction performances of the lightening process;
- 5) Effect of oil components on the shale oil lightening process;
- 6) In terms of mathematical modeling, models can be applied to predict the flow performance, considering the effects of T-H-M-C;
- 7) In terms of numerical simulation, the numerical model can indicate the flow law in both the nano-pore and the field scale.

4. Conclusions

This paper conducted experiments on the shale oil lightening process while varying parameters such as the heating rate, the reaction atmosphere and the presence of formation rock. From the results, four conclusions can be drawn:

- 1) In the shale oil lightening process, the air atmosphere indicates a complex reaction under high temperature, due to the oxidation reaction occurring during the process. Under a CO_2 atmosphere, the lightening reaction is more intense than that under other gas phases, and it gains the highest reaction rate because CO_2 provides the C component and promotes the H component as free radicals. Thus, the amount of hydrocarbons in the produced liquids is boosted.
- 2) Under higher temperature stages, the minerals in the formation rock act as catalyst in the shale oil lightening process. In the presence of formation rock, the reaction rate increases significantly in the mixture of rock and shale oil, and more light components are obtained in the lightened shale oil and the gas phase.
- 3) In the presence of formation rock under different heating

rates in the high-temperature CO₂ atmosphere, higher heating rate resulted in a higher lightening temperature area of the shale oil, and the higher lightening rate in the chemical reaction stage was investigated.

- 4) For the kinetic parameters of the lightening process, the proportional relationships between kinetic parameters and heating rates for lightening process in CO₂ atmosphere with and without formation rock were obtained, but the trends for the N₂ atmosphere were different.

Acknowledgements

The authors would like to acknowledge the financial support from the National Natural Science Foundation of China (No. 52374049), the Open Research Fund of State Key Laboratory of Geomechanics and Geotechnical Engineering Safety (No. SKLGME022029), and the Open Fund of State Key Laboratory of Oil and Gas Reservoir Geology and Exploitation (Southwest Petroleum University) (No. PLN202430),.

Conflict of interest

The authors declare no competing interest.

Open Access This article is distributed under the terms and conditions of the Creative Commons Attribution (CC BY-NC-ND) license, which permits unrestricted use, distribution, and reproduction in any medium, provided the original work is properly cited.

References

- Al-Harashsheh, M., Al-Ayed, O., Robinson, J., et al. Effect of demineralization and heating rate on the pyrolysis kinetics of Jordanian oil shales. *Fuel Processing Technology*, 2011, 92(9): 1805-1811.
- Alvarez, E., Marroquín, G., Trejo, F., et al. Pyrolysis kinetics of atmospheric residue and its SARA fractions. *Fuel*, 2011, 90(12): 3602-3607.
- Bagci, S., Kok, M. V. Combustion reaction kinetics studies of Turkish crude oils. *Energy & Fuels*, 2004, 18(5): 1472-1481.
- Belgrave, J. D. M., Moore, R. G., Ursenbach, M. G., et al. A comprehensive approach to *in-situ* combustion modeling. *SPE Advanced Technology Series*, 1993, 1(1): 98-107.
- Borrego, A. G., Prado, J. G., Fuente, E., et al. Pyrolytic behaviour of Spanish oil shales and their kerogens. *Journal of Analytical and Applied Pyrolysis*, 2000, 56(1): 1-21.
- Chang, Z., Chu, M. The chemical composition and pyrolysis characteristics of thermal bitumen derived from pyrolyzing huadian oil shale, China. *Oil Shale*, 2019, 36(1): 62-75.
- Chang, Z., Chu, M., Zhang, C., et al. Investigation of the effect of selected transition metal salts on the pyrolysis of Huadian oil shale, China. *Oil Shale*, 2017, 34(4): 354-367.
- Chang, Z., Chu, M., Zhang, C., et al. Comparison of pyrolysis characteristics of two Chinese oil shales based on the migration and conversion of organic carbon. *Carbon Resources Conversion*, 2018, 1(3): 209-217.
- Coats, A. W., Redfern, J. P. Kinetic parameters from thermogravimetric data. *Nature*, 1964, 201: 68-69.
- Eletsii, P. M., Mironenko, O. O., Kukushkin, R. G., et al. Catalytic steam cracking of heavy oil feedstocks: A review. *Catalysis in Industry*, 2018, 10(3): 185-201.
- Feng, Q., Xu, S., Xing, X., et al. Advances and challenges in shale oil development: A critical review. *Advances in Geo-Energy Research*, 2020, 4(4): 406-418.
- Gai, R., Jin, L., Zhang, J., et al. Effect of inherent and additional pyrite on the pyrolysis behavior of oil shale. *Journal of Analytical and Applied Pyrolysis*, 2014, 105: 342-347.
- Gao, Y., Li, Q., He, X., et al. Quantitative evaluation of shale-oil recovery during CO₂ huff-n-puff at different pore scales. *Energy & Fuels*, 2021, 35(20): 16607-16616.
- Gong, Y., Gu, Y. Miscible CO₂ simultaneous water-and-gas (CO₂-SWAG) injection in the Bakken formation. *Energy & Fuels*, 2015a, 29(9): 5655-5665.
- Gong, Y., Gu, Y. Experimental study of water and CO₂ flooding in the tight main pay zone and vuggy residual oil zone of a carbonate reservoir. *Energy & Fuels*, 2015b, 29(10): 6213-6223.
- Gu, J., Deng, S., Sun, Y., et al. Pyrolysis behavior and pyrolysate characteristics of Huadian oil shale kerogen catalyzed by nickel-modified montmorillonite. *Advances in Geo-Energy Research*, 2024, 11(3): 168-180.
- Guo, Q., Hou, L., Wang, J., et al. An evaluation method of resource potential of *in-situ* converted shale oil and its application. *Acta Prtrolei Sinica*, 2022, 43(12): 1750-1757. (in Chinese)
- Guo, W., Deng, S., Sun, Y. Recent advances on shale oil and gas exploration and development technologies. *Advances in Geo-Energy Research*, 2024a, 11(2): 81-87.
- Guo, W., Sun, Y., Li, Q., et al. Oil shale *in-situ* conversion technology triggered by topochemical reaction method and pilot test project in Songliao Basin. *Acta Prtrolei Sinica*, 2024b, 45(7): 1104-1121. (in Chinese)
- Hao, J., Feng, W., Qiao, Y., et al. Thermal cracking behaviors and products distribution of oil sand bitumen by TG-FTIR and Py-GC/TOF-MS. *Energy Conversion and Management*, 2017, 151: 227-239.
- He, L., Ma, Y., Yue, C., et al. The heating performance and kinetic behaviour of oil shale during microwave pyrolysis. *Energy*, 2022, 244: 123021.
- Jaber, J. O., Probert, S. D. Pyrolysis and gasification kinetics of Jordanian oil-shales. *Applied Energy*, 1999, 63: 269-286.
- Jaber, J. O., Probert, S. D., Williams, P. T., et al. Gasification potential and kinetics of Jordanian oil shales using CO₂ as the reactant gas. *Energy Sources*, 2000, 22(6): 573-585.
- Jia, B., Tsau, J. S., Barati, R. A review of the current progress of CO₂ injection EOR and carbon storage in shale oil reservoirs. *Fuel*, 2019, 236: 404-427.
- Jiang, H., Deng, S., Chen, J., et al. Effect of hydrothermal pretreatment on product distribution and characteristics of oil produced by the pyrolysis of Huadian oil shale. *Energy Conversion and Management*, 2017, 143: 505-512.
- Jiang, H., Liu, S., Wang, J., et al. Study on evolution mech-

- anism of the pyrolysis of chang 7 oil shale from Ordos basin in China. *Energy*, 2023, 272: 127097.
- Jin, L., Hawthorne, S., Sorensen, J., et al. Advancing CO₂ enhanced oil recovery and storage in unconventional oil play—Experimental studies on Bakken shales. *Applied Energy*, 2017, 208: 171-183.
- Kang, Z., Zhao, Y., Yang, D. Review of oil shale *in-situ* conversion technology. *Applied Energy*, 2020, 269: 115121.
- Kapadia, P. R., Wang, J., Kallos, M. S., et al. Practical process design for *in situ* gasification of bitumen. *Applied Energy*, 2013, 107: 281-296.
- Kim, D. W., Lee, C. H. Efficient conversion of extra-heavy oil into distillates using tetralin/activated carbon in a continuous reactor at elevated temperatures. *Journal of Analytical and Applied Pyrolysis*, 2019, 140: 245-254.
- Kök, M. V., Karacan, O. Pyrolysis analysis and kinetics of crude oils. *Journal of Thermal Analysis and Calorimetry*, 1998, 52: 781-788.
- Lan, X., Luo, W., Song, Y., et al. Effect of the temperature on the characteristics of retorting products obtained by Yaojie oil shale pyrolysis. *Energy & Fuels*, 2015, 29(12): 7800-7806.
- Liu, D., Hou, J., Luan, H., et al. Coke yield prediction model for pyrolysis and oxidation processes of low-asphaltene heavy oil. *Energy & Fuels*, 2019, 33(7): 6205-6214.
- Liu, Z., Meng, Q., Dong, Q., et al. Characteristics and resource potential of oil shale in China. *Oil Shale*, 2017, 34(1): 15-41.
- Maniscalco, M., Mistretta, L., Iannotta, P., et al. Experimental study of the pyrolysis of waste bitumen for oil production. *Journal of the Energy Institute*, 2020, 93(6): 2456-2463.
- Meng, X., Bian, J., Li, J., et al. Porous aluminosilicates catalysts for low and medium matured shale oil *in situ* upgrading. *Energy Science and Engineering*, 2020, 8(8): 2859-2867.
- Moine, E. C, Groune, K., El Hamidi, A., et al. Multistep process kinetics of the non-isothermal pyrolysis of Moroccan Rif oil shale. *Energy*, 2016, 115: 931-941.
- Mozaffari, S., Järvi, O., Baird, Z. S. Effect of N₂ and CO₂ on shale oil from pyrolysis of Estonian oil shale. *International Journal of Coal Preparation and Utilization*, 2022, 42(10): 2908-2922.
- Murugan, P., Mani, T., Mahinpey, N., et al. Pyrolysis kinetics of Athabasca bitumen using a TGA under the influence of reservoir sand. *Canadian Journal of Chemical Engineering*, 2012, 90(2): 315-319.
- Ogbonnaya, O., Suriamin, F., Shiau, B., et al. Enhanced oil recovery formulations for liquid-rich shale reservoirs. *Fuel*, 2024, 368: 131573.
- Pan, L., Dai, F., Huang, J., et al. Study of the effect of mineral matters on the thermal decomposition of Jimsar oil shale using TG-MS. *Thermochimica Acta*, 2016, 627-629: 31-38.
- Pan, L., Dai, F., Li, G., et al. A TGA/DTA-MS investigation to the influence of process conditions on the pyrolysis of Jimsar oil shale. *Energy*, 2015, 86: 749-757.
- Pu, W., Gong, X., Chen, Y., et al. Non-isothermal pyrolysis and combustion kinetics of heavy oil and its low temperature oxidation products by thermal analyses. *Petroleum Science and Technology*, 2020, 38(4): 398-404.
- Quan, H., Xing, L. The effect of hydrogen bonds between flow improvers with asphaltene for heavy crude oil. *Fuel*, 2019, 237: 276-282.
- Raja, M. A., Zhao, Y., Zhang, X., et al. Practices for modeling oil shale pyrolysis and kinetics. *Reviews in Chemical Engineering*, 2017, 34(1): 21-42.
- Ren, Y., Freitag, N. P., Mahinpey, N. A simple kinetic model for coke combustion during an *in situ* combustion (ISC) process. *Journal of Canadian Petroleum Technology*, 2007, 46(4): 47-52.
- Ren, Y., Wei, B., Ji, B., et al. Pore-scale probing CO₂ huff-n-puff in extracting shale oil from different types of pores using online T1-T2 nuclear magnetic resonance spectroscopy. *Petroleum Science*, 2024, 21(6): 4119-4129.
- Shabib-Asl, A., Plaksina, T., Moradi, B. Evaluation of nanopore confinement during CO₂ huff and puff process in liquid-rich shale formations. *Computational Geosciences*, 2020, 24(3): 1163-1178.
- Syed, S., Qudaih, R., Talab, I., et al. Kinetics of pyrolysis and combustion of oil shale sample from thermogravimetric data. *Fuel*, 2011, 90: 1631-1637.
- Tang, L., Yan, Y., Meng, Y., et al. CO₂ gasification and pyrolysis reactivity evaluation of oil shale. *Energy Procedia*, 2019, 158: 1694-1699.
- Wang, L., Gao, C., Xiong, R., et al. Development review and the prospect of oil shale *in-situ* catalysis conversion technology. *Petroleum Science*, 2024, 21(2): 1385-1395.
- Williams, P. T., Ahmad, N. Investigation of oil-shale pyrolysis processing conditions using thermogravimetric analysis. *Applied Energy*, 2000, 66(2): 113-133.
- Xie, F., Wang, Z., Lin, W., et al. Study on thermal conversion of huadian oil shale under N₂ and CO₂ atmospheres. *Oil Shale*, 2010, 27(4): 309-320.
- Yang, Q., Zhang, X., Xu, S., et al. Low-temperature co-current oxidizing pyrolysis of oil shale: Study on the physicochemical properties, reactivity and exothermic characters of semi-coke as heat generation donor. *Journal of Petroleum Science and Engineering*, 2022a, 216: 110726.
- Yang, S., Huang, S., Jiang, Q., et al. Experimental study of hydrogen generation from *in-situ* heavy oil gasification. *Fuel*, 2022b, 313: 122640.
- Yuan, C., Emelianov, D. A., Varfolomeev, M. A. Oxidation behavior and kinetics of light, medium, and heavy crude oils characterized by thermogravimetry coupled with fourier transform infrared spectroscopy. *Energy & Fuels*, 2018, 32(4): 5571-5580.
- Yu, H., Xu, H., Fu, W., et al. Extraction of shale oil with supercritical CO₂: Effects of number of fractures and injection pressure. *Fuel*, 2021, 285: 118977.
- Zhang, C., Xu, T., Shi, H., et al. Physicochemical and pyrolysis properties of SARA fractions separated from asphalt binder. *Journal of Thermal Analysis and Calorimetry*, 2015, 122(1): 241-249.
- Zhao, Q., Dong, Y., Zheng, L., et al. Sub- and supercritical

- water conversion of organic-rich shale with low-maturity for oil and gas generation: Using Chang 7 shale as an example. *Sustainable Energy and Fuels*, 2022, 7(1): 155-163.
- Zhao, S., Lü, X., Li, Q., et al. Thermal-fluid coupling analysis of oil shale pyrolysis and displacement by heat-carrying supercritical carbon dioxide. *Chemical Engineering Journal*, 2020, 394: 125037.
- Zhao, W., Guan, M., Liu, W., et al. Low-to-medium maturity lacustrine shale oil resource and *in-situ* conversion process technology: Recent advances and challenges. *Advances in Geo-Energy Research*, 2024, 12(2): 81-88.
- Zhao, W., Hu, S., Hou, L. Connotation and strategic role of *in-situ* conversion processing of shale oil underground in the onshore China. *Petroleum Exploration and Development*, 2018, 45(4): 563-572.
- Zhao, X., Sang, Q., Li, Y., et al. CO₂-kerogen interaction dominated CO₂-oil counter-current diffusion and its effect on ad-/absorbed oil recovery and CO₂ sequestration in shale. *Fuel*, 2021, 294: 120500.
- Zhou, J., Yang, K., Zhou, L., et al. Microstructure and mechanical properties alterations in shale treated via CO₂/CO₂-water exposure. *Journal of Petroleum Science and Engineering*, 2021, 196: 108088.
- Zhou, X., Li, X., Shen, D., et al. CO₂ huff-n-puff process to enhance heavy oil recovery and CO₂ storage: An integration study. *Energy*, 2022, 239: 122003.